AIP | Applied Physics Letters

Tin doped indium oxide core—TiO2 shell nanowires on stainless steel mesh for flexible photoelectrochemical cells

Jun Hong Noh, Bo Ding, Hyun Soo Han, Ju Seong Kim, Jong Hoon Park, Sang Baek Park, Hyun Suk Jung, Jung-Kun Lee, and Kug Sun Hong

Citation: Applied Physics Letters **100**, 084104 (2012); doi: 10.1063/1.3684805
View online: http://dx.doi.org/10.1063/1.3684805
View Table of Contents: http://scitation.aip.org/content/aip/journal/apl/100/8?ver=pdfcov
Published by the AIP Publishing

Tin doped indium oxide core—TiO_2 shell nanowires on stainless steel mesh for flexible photoelectrochemical cells

Jun Hong Noh,[1] Bo Ding,[2] Hyun Soo Han,[3] Ju Seong Kim,[3] Jong Hoon Park,[3] Sang Baek Park,[3] Hyun Suk Jung,[4] Jung-Kun Lee,[2,a)] and Kug Sun Hong[3,a)]
[1]*KRICT-EPFL Global Research Laboratory, Advanced Materials Division, Korea Research Institute of Chemical Technology, Daejeon 305-600, Korea*
[2]*Department of Mechanical Engineering and Materials Science, University of Pittsburgh, Pittsburgh, Pennsylvania 15261, USA*
[3]*WCU Hybrid Materials Program, Department of Materials Science and Engineering, Seoul National University, Seoul 151-744, Korea*
[4]*School of Advanced Materials Science and Engineering, Sungkyunkwan University, Suwon 440-746, Korea*

(Received 31 October 2011; accepted 23 January 2012; published online 23 February 2012)

Photoanode architecture is built on highly conductive tin doped indium oxide (ITO) nanowires (NWs) on a flexible stainless steel mesh (SSM). ITO nanowires were coated with the atomic layer deposition grown TiO_2 layer and the photoelectrochemical performance of the stainless steel mesh based photoanode were examined as a function of wire-length and shell-thickness. The photoanode consisting of 20 μm-long nanowire core and 36 nm thick shell increased the photocurrent of the testing cell by 4 times, compared to a reference cell. This enhanced photochemical activity is attributed to higher light harvesting efficiency of nanowire arrays and suppressed charge recombination of core-shell structure. © *2012 American Institute of Physics*. [doi:10.1063/1.3684805]

A photoelectrochemical (PEC) cell has emerged due to its capability to convert solar radiation into useful forms of energy such as hydrogen[1] without leaving carbon dioxide.[2] In this field, one of the most critical issue is the enhancement of light-harvesting and charge collection in photoanodes to achieve efficient conversion performance in PEC cell.[3–5] A great amount of efforts are being devoted to developing photoanodes (i.e., increasing surface area and reducing band gap of semiconductors) to effectively harvest more visible light.[6–9] However, currently available devices still exhibit moderate performance, due to the short hole diffusion length and the trade-off relationship between surface area and charge collection.[10–12]

Highly conductive oxide *core*-thin photoanode materials *shell* nanowire (NW) structure can be a solution to the problems associated surface area and charge collection. First, a NW array has large surface area, compared with a flat film. Second, a thin shell layer of several tens nanometer on the surface of NWs provides a path for the transport of photogenerated electrons and holes with minimized recombination.[13–15] Herein, we demonstrated the core-shell NW type photoanode with very large surface area by growing highly conductive In_2O_3:Sn (ITO) *core*-atomic layer deposited TiO_2 *shell* NWs on flexible stainless steel mesh (SSM) substrate. ITO NWs which were directly synthesized on SSM without any catalysts offered both large surface area and rapid electron conducting path. A flexible core-shell NWs photoelectrodes on SSM showed fourfold higher photocurrent than bare SSM photoelectrode. In addition, it was found that the photoanode on highly flexible SSM substrates can be installed onto non-planar surface, because of the rolling ability of SSM.

Figures 1(a)–1(c) shows scanning electron microscopy (SEM) images of bare, ITO NWs-SSM, and ITO-NWs, respectively. SSM (wire diameter of 28 μm, 325 mesh) with an open area of 41% shown in Fig. 1(a) was used as a flexible conducting substrate. On the SSM, ITO NWs were grown by a vapor transport method (VTM) using a tube furnace. High-purity (99.99%) metallic indium and tin powders were mixed thoroughly in an atomic ratio of 10:3. The mixture, loaded in a fused silica boat, was located at the center of a

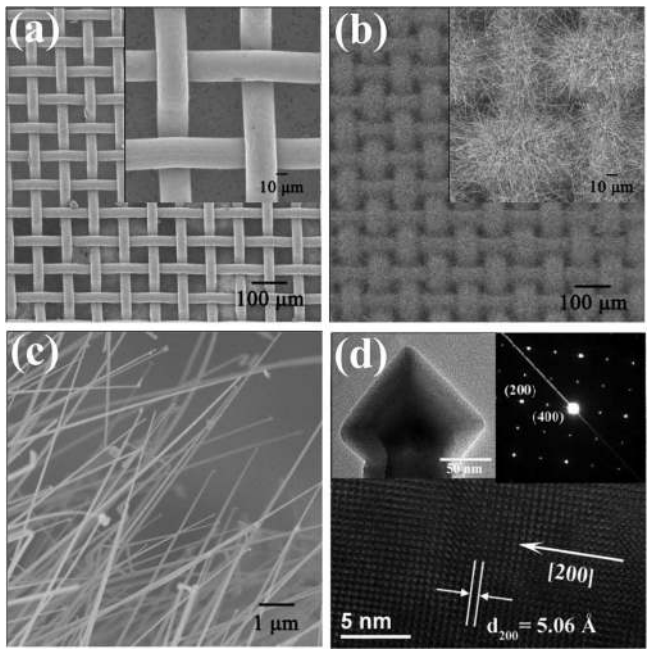

FIG. 1. SEM images of (a) bare-stainless steel mesh (SSM) substrate, (b) ITO-NWs on SSM, and (c) ITO NW. Inserts are high magnitude SEM images. (d) HRTEM image of ITO NW and inserts are TEM image of NW-tip and selective area diffraction (SAD) pattern.

[a)]Authors to whom correspondence should be addressed. Electronic addresses: jul37@pitt.edu and kshongss@plaza.snu.ac.kr.

fused silica tube and the SSM was then positioned several centimeters from the mixture powder. The ITO NWs were grown at 800 °C while maintaining the pressure inside the tube below 1.5×10^{-3} Torr by introducing the oxygen gas to the tube with a flow rate of 10 sccm during the growth process.

As shown in Figs. 1(b) and 1(c), ITO NWs were conformally formed on the interwoven wire array of the SSM. A length of ITO NWs is in the range of $10 \sim 40\ \mu$m, depending on the growth time. A mean diameter of ITO NWs was less than $50 \sim 200$ nm and their aspect ratio was larger than 100. In contrast to the well-known Au catalyst facilitated vapor-liquid-solid (VLS) growth mode,[16] we grew ITO NWs without using any catalyst. Catalyst-free growth of ITO nanowire on various substrates has been explained by seed formation of In_2O_3 octahedrons[17–19] or Sn-In alloy droplets.[20] A SEM image in Fig. 1(c) and a transmission electron microscopy (TEM) image in Fig. 1(d) show that the end of ITO NWs has an octahedron shape particle. Its similarity to recently reported In_2O_3 NWs suggests that octahedron seeds were formed first on the SSM and ITO NWs were grown along the seeds via a vapor-solid (VS) mode.[17,18] Therefore, a uniform ITO NW array was synthesized conformally on the stainless steel wires, without the limitation of catalyst pretreatment. High resolution transmission electron microscopy (HRTEM) image and the selective area diffraction (SAD) pattern with a zone axis of [020] of an ITO NW shows that the single-crystalline ITO NWs grew perfectly along [200] direction. The electric conductivity of the ITO NW was measured as high as $2.0 \times 10^3\ S \cdot cm^{-1}$ in our previous report, due to appropriate doping level of Sn in ITO NWs.[15]

Figure 2(a) presents a schematic of a flexible photoelectrode. The photoelectrode of ITO NWs built on the SSM can be easily bent. In addition, highly conductive ITO NW 3-D array architecture is expected to offer rapid electron transport pathway as well as large surface area which are the requirements for highly efficient photocatalytic reaction. To examine the performance of the photoelectrode in water splitting, TiO_2 shell layers were coated on the surface of ITO NWs as a light absorbing layer. TiO_2 coating was performed at 250 °C by the atomic layer deposition (ALD) technique. Titanium isopropoxide and H_2O were used as Ti-source and oxidant, respectively. The thickness of the TiO_2 shell layer ranged from 15 to 45 nm. A conformal coating of TiO_2 layer on ITO NWs was observed in a TEM image of Fig. 2(b) and cross-sectional TEM image of Fig. 2(c). The high-resolution TEM image of the TiO_2 shell layer in Fig. 2(d) reveals that the as-deposited TiO_2 shell is high crystalline anatase. The atomic spacing is 0.35 nm which coincides with that of (101) plane of anatase phase. In addition, the fast Fourier transformation (FFT) pattern of the shell layer in the insert of Fig. 2(d) presents a diffraction pattern corresponding to the (101) plane of anatase TiO_2.

Photoelectrochemical measurements were performed in a three-electrode electrochemical cell. A NW arrays on SSM was used as a working electrode. A counter electrode was a platinum plate and a reference electrode was a saturated calomel electrode (SCE). A UV light source was a 450 W mercury arc lamp and an electrolyte was 1 M KOH solution. Area of a photoanode immersed in the electrolyte was 1 cm^2.

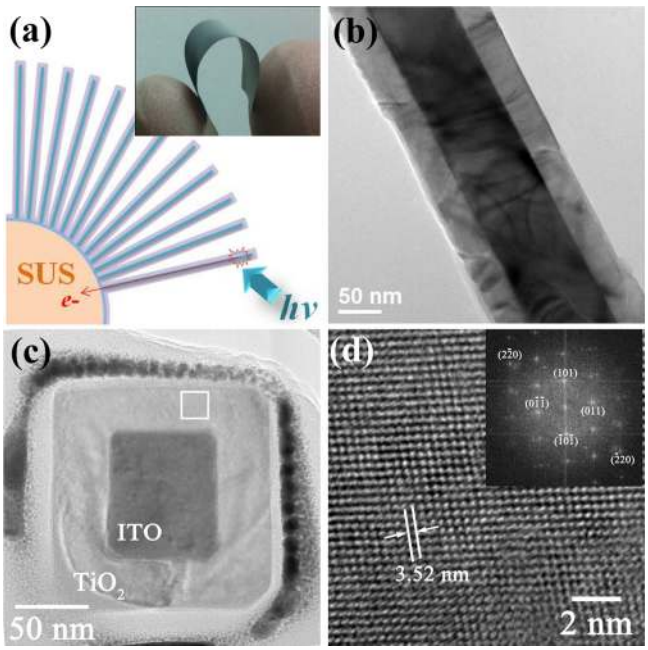

FIG. 2. (Color online) (a) Scheme of ITO core-TiO_2 shell NW photoanode structure on SSM and practical picture of the bended photoanode; TEM image (b) and a cross-sectional TEM image (c) of ITO core-TiO_2 shell NWs; and (d) HRTEM image of TiO_2 shell layer and its FFT pattern.

Before the measurement, the electrochemical cell was deaerated by purging nitrogen gas. The photocurrent density—applied potential (*J-V*) curves for ITO NWs with a 36 nm-thick TiO_2 shell layer are presented in Fig. 3(a) as a function of NW length. Dark current density of all samples was negligible. Large negative onset potential about −1.0 V vs SCE was observed. A slope of *J-V* curves was steep at low applied bias, regardless of NW length, compared to previous studies using similar measurement conditions.[21,22] Similar onset potential and steep slope of the cells with different NW length indicates that the electrons photoexcited within TiO_2 shell are effectively collected to ITO and transport mainly through highly conductive ITO core. In the core-shell structure, photogenerated electrons in TiO_2 travel through the shell layer before they are collected by ITO core. Hence, the electron mean free path within TiO_2 shell is shorter than 36 nm, which is not influenced by NW length.

It is noted that photocurrent densities of ITO NW-SSM samples at 0 V vs SCE are 4 times higher than that of bare SSM sample and the enhanced photocurrent density is saturated above ITO NW length of 20 μm. Higher photocurrent of ITO NW-SSM samples can be explained by the larger surface and light trapping effect of the NW structure. The increased surface area of NW array grown SSM promotes the photochemical reaction on the surface of TiO_2 and enhance photocurrent density. However, although surface area of TiO_2 increases with increasing NW length, photocurrent density does not increase any more above length of 20 μm. In addition to the surface area, NW arrays on SSM were found to traps incoming light. The transmittance (T, %) and reflectance (R, %) of samples at a wavelength 360 nm were measured by a quantum efficiency measurement system (QE-1100, Otsuka Electronics Co.) with an integrated semisphere. As shown in Fig. 3(b), the ITO NW array on SSM

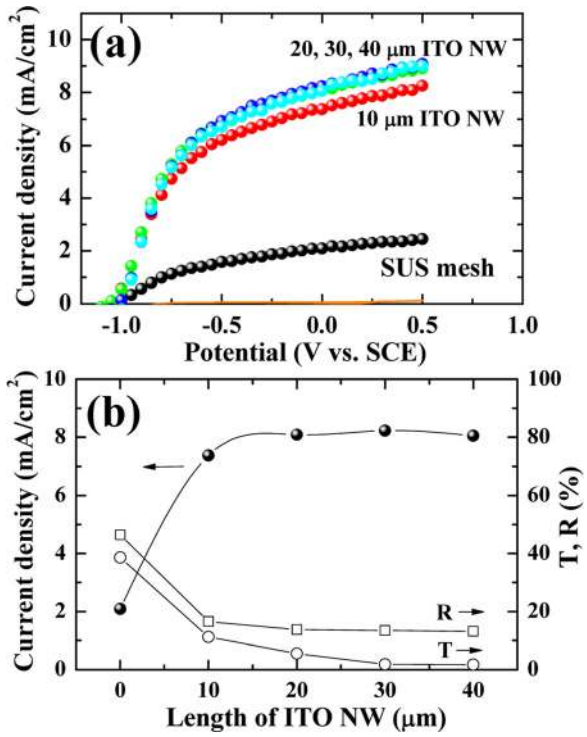

FIG. 3. (Color online) (a) Current density vs applied potential (J-V) characteristics of the core-shell photoanodes as a function of ITO NW length, the orange line indicates dark currents of all the specimens. (b) Current density at 0 V vs SCE, transmittance and reflectance at 360 nm of the core-shell photoanodes as a function of ITO NW length.

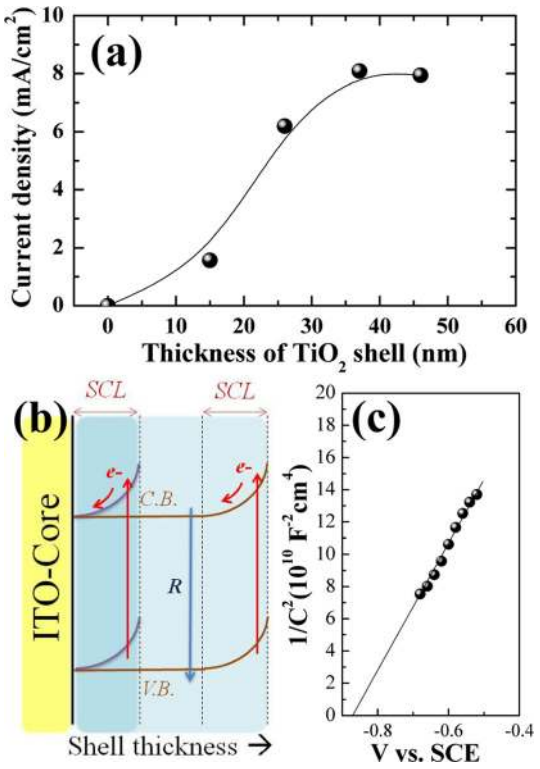

FIG. 4. (Color online) (a) Current density at 0 V vs SCE of the core-shell photoanodes as a function of TiO_2 shell thickness. (b) Conduction band (C.B.) and valance band (V.B.) bending scheme within shell layers thin or thicker than SPL thickness. (c) Mott-Schottky plot of 50 nm-thick ALD-TiO_2 film at the frequency of 10 kHz.

reduced both transmittance and reflectance. The SSM sample without NWs loses 80% of incoming photons via reflection and transmission. In contrast, NWs longer than 20 μm significantly decreased the transmittance (<5%) and reflectance (~13%). This attests to the fact that the photoanodes absorbs more than 80% of incoming photons with an assistance of a light trapping effect. An increase in the light absorption by 3 times is consistent with an increase in the photocurrent by 4 times, which also implies that the carrier recombination within NWs is negligible. As the length of NWs becomes larger than 20 μm, the reflectance and transmittance of the samples are saturated. This shows that ITO-TiO_2 core-shell NWs with length of 20 μm are long enough to fully harvest UV light used in our study.

In addition to the length of ITO NW, the effect of TiO_2 shell thickness was examined to maximize the photoexcitation of carriers and minimize the carrier recombination. Figure 4(a) shows photocurrent density for the photoanode of ITO-TiO_2 core-shell NWs on the SSM as a function of TiO_2 shell thickness. The length of NWs was fixed at 20 μm. The photocurrent density increased until TiO_2 shell thickness reaches 35 nm. An increase in the photocurrents is not observed between 35 nm thick TiO_2 shell and 45 nm thick TiO_2 shell samples. Since thicker TiO_2 layer absorbs more photons, the saturated photocurrent indicates that additionally generated photocarriers in the thicker TiO_2 layer are dissipated via the recombination. At the interface between TiO_2 and electrolyte, a built-in-potential of a space charge layer (SCL) region plays a major role in separating photogenerated electrons from TiO_2 to ITO. Therefore, the increase in the carrier recombination of the thicker TiO_2 shell indicates that a significant portion of carriers are produced outside SCL region. These electrons have higher chance of the recombination, due to absence of the built-up potential.[23,24] As shown in Fig. 4(b), therefore, thicker shell layer than SCL thickness might not be needed to increase photocurrent due to the bulk recombination. SCL thickness formed in shell layer is an optimal shell thickness for the PEC cell.

The SCL thickness depends on dielectric constant and donor density of the prepared film and it can be derived from the Mott-Schottky plot relationship.[25] To estimate the SCL thickness of the ALD-TiO_2 layer, 50 nm-thick TiO_2 film specimens on ITO substrate were prepared. Figure 4(b) represents the Mott-Schottky plot of the TiO_2 film on ITO/glass substrate with area of $1 \times 1\,cm^2$ by following Eq. (1) which was measured at 10 kHz using an electrochemical analyzer (CHI-608C, CH Instruments).

$$\frac{1}{C_{SC}^2} = \frac{2}{\varepsilon\varepsilon_0 e N_D}\left(V - V_{fb} - \frac{kT}{e}\right), \tag{1}$$

where C_{SC} is the capacitance of the sound pressure level (SPL), ε is the dielectric constant of anatase, ε_0 is the vacuum permittivity, e is the elementary charge, N_D denotes the donor density, V_{fb} is the flat band potential, k is Boltzmann constant, and T is Kelvin degree. The slope determined from the analysis of Mott-Schottky plot were used to estimate the carrier density using Eq. (2).

$$N_D = \frac{2}{\varepsilon\varepsilon_0 e}\left[\frac{d(1/C^2)}{dV}\right]^{-1}. \tag{2}$$

With an experimentally measured ε, 71 for the ALD grown TiO_2 film, the electron density of ALD-TiO_2 film was then calculated to be $4.52 \times 10^{18}\,cm^{-3}$. The thickness of the SPL at TiO_2 surface can also be derived from the Mott-Schottky plot relationship[26]

$$d_{SC} = \left(\frac{2\varepsilon\varepsilon_0}{eN_D}\right)^{1/2}\left(V - V_{fb} - \frac{kT}{e}\right)^{1/2}. \quad (3)$$

The calculated thickness of SCL at 0 V vs SCE for the ALD-TiO_2 thin film is 36.8 nm, which is similar to previous reports that SCL thickness of anatase is range in several tens nanometer.[24,27,28] The saturated photocurrent above 35 nm can be explained by the obtained SCL thickness of 36.8 nm.

In conclusion, we fabricated flexible photoanode combined highly conductive ITO core-thin TiO_2 shell layer NW array with SSM substrate. ITO NWs were synthesized on the SSM without any catalysts by a VTM process. A conformal TiO_2 shell layer was subsequently deposited on ITO NWs by an ALD process. The core-shell NW array on SSM offered large surface area and enhanced light trapping, which increase the photocurrent of the electrochemical cell by 4 times. As the length of NWs became larger than 20 μm, the light absorption and the photocurrent were saturated. The charge transfer from TiO_2 to ITO was explained by the built-in potential in SCL region of TiO_2. An experimentally determined critical thickness of TiO_2 shell, 36 nm was consistent with the theoretical prediction based on Mott-Schottky relationship and carrier depletion. The flexible core-shell photoanode structure in this study provides important insights into the design of highly efficient photoanode with enhanced charge collection and light harvesting.

This work was supported by the National Research Foundation of Korea (NRF) grant funded by the Korea government (MEST) (2009-0092779) and WCU (World Class University) program through National Research Foundation of Korea funded by the Ministry of Education, Science and Technology (R31-2008-000-10075-0).(RIAM) Authors in the University of Pittsburgh acknowledge the support from National Science Foundation (Grant No. DMR-0847319).

[1]A. Fujishima and K. Honda, Nature **238**, 37 (1972).
[2]M. Halmann, Nature **275**, 115 (1978).
[3]Y. J. Hwang, A. Boukai, and P. Yang, Nano Lett. **9**, 410 (2009).
[4]G. Wang, H. Wang, Y. Ling, Y. Tang, X. Yang, R. C. Fitzmorris, C. Wang, J. Z. Zhaong, and Y. Li, Nano Lett. **11**, 3026 (2011).
[5]S.-T. Bae, H. Shin, J. Y. Kim, H. S. Jung, and K. S. Hong, J. Phys. Chem. C **112**, 9937 (2008).
[6]M. Zhang, W. Luo, Z. Li, T. Yu, and Z. Zou, Appl. Phys. Lett. **97**, 042105 (2010).
[7]X. Peng, K. Shankar, O. K. Varghese, M. Paulose, T. J. Latempa, and C. A. Grimes, Nano Lett. **8**, 3781 (2008).
[8]I. Cesar, A. Kay, J. A. G. Martinez, and M. Gratzel, J. Am. Chem. Soc. **128**, 4582 (2006).
[9]Y. Hou, X.-Y. Li, Q.-D. Zhao, X. Quan, and G.-H. Chen, Adv. Funct. Mater. **20**, 2165 (2010).
[10]Y. Lin, G. Yuan, R. Liu, S. Zhou, S. W. Sheehan, and D. Wang, Chem. Phys. Lett. **507**, 209 (2011).
[11]A. Kay, I. Cesar, and M. Gratzel, J. Am. Chem. Soc. **128**, 15714 (2006).
[12]P. Lianos, J. Hazard. Mater. **185**, 575 (2011).
[13]Y. Lin, S. Zhou, X. Liu, S. W. Sheehan, and D. Wang, J. Am. Chem. Soc. **131**, 2773 (2009).
[14]Y. Lin, S. Zhou, S. W. Sheehan, and D. Wang, J. Am. Chem. Soc. **133**, 2398 (2011).
[15]J. H. Noh, H. S. Han, S. Lee, J. Y. Kim, K. S. Hong, G.-S. Han, H. Shin, and H. S. Jung, Adv. Energy Mater. **1**, 829 (2011).
[16]Q. Wan, M. Wei, D. Zhi, J. L. MacManus-Driscoll, and M. G. Blamire, Adv. Mater. **18**, 234 (2006).
[17]Y. Yan, Y. Zhang, H. Zeng, J. Zhang, X. Cao, and L. Zhang, Nanotechnology **18**, 175601 (2007).
[18]W. Yin, M. Cao, S. Luo, C. Hu, and B. Wei, Cryst. Growth Des. **9**, 2173 (2009).
[19]N. Wan, J. Xu, G. Chen, X. Gan, S. Guo, L. Xu, and K. Chen, Acta Mater. **58**, 3068 (2010).
[20]Y. Q. Chen, J. Jiang, B. Wang, and J. G. Hou, J. Phys. D: Appl. Phys. **37**, 3319 (2004).
[21]Y. Su, S. Chen, X. Quan, H. Zhao, and Y. Zhang, Appl. Surf. Sci. **255**, 2167 (2008).
[22]N. Lu, X. Quan, J. Y. Li, S. Chen, H. T. Yu, and G. H. Chen, J. Phys. Chem. C **111**, 11836 (2007).
[23]M. Takahashi, K. Tsukigi, T. Uchino, and T. Yoko, Thin Solid Films **388**, 231 (2001).
[24]C. A. Grimes, J. Mater. Chem. **17**, 1451 (2007).
[25]F. Cardon and W. P. Gomes, J. Phys. D: Appl. Phys. **11**, L63 (1978).
[26]W. Z. Schottky, Phys. **118**, 539 (1942).
[27]M. Radecka, M. Wierzbicka, and M. Rekas, Physica B **351**, 121 (2004).
[28]F. Fabregat-Santiago, G. Garcia-Belmonte, J. Bisquert, P. Bogdanoff, and A. Zaban, J. Electrochem. Soc. **150**, E293 (2003).